JOURNAL OF CATALYSIS 144, 77–92 (1993)

Processes in MoS_2 Gasification

X. CHU AND L. D. SCHMIDT[1]

Department of Chemical Engineering and Materials Science, University of Minnesota, Minneapolis, Minnesota 55455

Received November 30, 1992; revised June 21, 1993

The gasification of MoS_2 by H_2 has been studied by scanning tunneling microscopy (STM) and atomic force microscopy (AFM). Two fundamental processes were found upon heating the (0001) surface of MoS_2 in H_2: first, the surface sulfur layer is removed from some defect sites on the MoS_2 basal plane to form monolayer pits, and second, the exposed Mo layer forms small clusters which catalyze the further gasification of the sulfur layer, thus enhancing the number of edge atoms. At low reaction pressures, these two processes remove mainly the top sandwich layer and no Mo particles channel into the top sulfur layer. However, at high pressure or temperature, the gasification is dominated by the motion of the Mo particles which then produce high-density channel structures on the surface. Adding thiophene to H_2 retards the gasification of MoS_2, suggesting the active catalytic sites are the atoms at the steps on the surface. Ni and Co catalyze the gasification of MoS_2 and greatly increase the total number of edge sites. © 1993 Academic Press, Inc.

INTRODUCTION

The presence of sulfur in crude oil and in coal-derived fuel causes two serious problems: first, sulfur-containing fuels cause air pollution; and, second, sulfur poisons catalysts in oil refining and in automotive catalytic converters. Therefore, sulfur removal in hydrodesulfurization (HDS) is carried out as one of the primary steps in petroleum processing.

Industrially, Mo–Co or Mo–Ni catalysts supported on Al_2O_3 are used to treat crude oil with hydrogen. The catalyst is prepared as oxides and is usually presulfurized to achieve good activities. Many researchers have studied this catalyst and the catalytic process (*1–7*). Several models have already been proposed based on various structural and surface analyses and good reviews have appeared (*3–5*). However, there has not been a unique picture of the catalytic operation thus far due to the lack of direct experimental evidence and the difficulties in evaluating the real system, especially changes in the catalyst surface. In order to design the best catalysts, details of active sites and their generation (i.e., the dynamic processes of the catalytic operation) are needed.

Defect structures in MoS_2 have been studied by gold decoration TEM as early as the late 1960s (*8, 9*). Coke deposition on MoS_2 has also been studied by the same technique (*10*). Because it is a good electrical conductor and a layered compound, MoS_2 has recently been studied extensively by STM for its structural and electronic properties (*11–17*).

STM has been used to study graphite oxidation and graphite-supported metal particles in different chemical environments (*18–21*). Recently, we have studied the gasification processes of graphite with various gases such as O_2, H_2, H_2O, CO_2, NO_x, and SO_2. STM is a unique way of studying these reactions quantitatively, because kinetics of these reactions can be obtained by examining the reacted surfaces of the sample after reacting at different temperatures, pressures, and times (*22–25*). We also studied the catalytic gasification of graphite by metals, oxides, and carbonates in various systems by STM and AFM (*24*).

STM and AFM have also been used to

[1] To whom correspondence should be addressed.

0021-9517/93 $5.00
Copyright © 1993 by Academic Press, Inc.
All rights of reproduction in any form reserved.

study the layer-by-layer etching of two-dimensional chalcogenides (*26, 27*) and the wearing of the oxided surface of MoS_2 (*28, 29*). However, properties which are related to its most important application as catalyst for HDS, such as the stability of this material or gasification behaviors of MoS_2 during reactions, have not been studied so far.

In this paper we present STM and AFM studies of the processes of MoS_2 gasification under both reducing and oxidizing atmospheres. The former is related to the most important application of this material in petroleum processing (i.e., hydrotreating), while the latter is related to the regeneration of this catalyst between periodic operations.

STM and AFM are unique techniques for detection of atomic structural changes on the basal plane of MoS_2. We found that two catalytic processes occurred on the basal plane of MoS_2 during H_2 gasification: first, the surface sulfur layer was removed from some defect sites to form monolayer pits, and, second, the exposed Mo layer formed smaller clusters which catalyzed the further gasification of the sulfur layer thus producing many more edge atoms.

By introduction of thiophene into the reaction system, we found that thiophene retards the gasification of MoS_2. This is consistent with the solid-state chemistry model (*30, 31*) that the hydrodesulfurization process occurs at the edge sites, with sulfur deposition by thiophene balancing the removal of sulfur by hydrogen. We also studied the promotion effects of Co and Ni on the reaction. We found that Ni and Co as catalysts accelerate the self-catalyzed gasification of MoS_2 in this process with Co having a relatively higher activity than Ni in catalyzing the gasification of MoS_2.

EXPERIMENTAL PROCEDURES

Natural MoS_2 single crystals from Anhui, China, were used in this study. Figure 1 shows an optical micrograph of a sample which had typical dimensions of 20 × 20 × 0.2 mm. For all noncatalytic reactions, freshly cleaved samples with dimensions of 5 × 5 × 0.1 mm were heated in a mixture of either 10% H_2 in He or 99.998% H_2 at atmospheric pressure at specified temperatures and times.

For Ni and Co catalyzed reactions, high purity Ni (99.99%) and Co (99.98%) metals were vacuum deposited on freshly cleaved samples. The samples were then heated in high purity He (99.995%) at 450°C for 2 h to convert the deposited thin metal films into small particles. The samples with Ni and Co were then heated in pure H_2 or a mixture of 10% H_2 in He at atmospheric pressure at specified temperatures and times. For reactions involving thiophene, pure H_2 or 10% H_2 in He was used to introduce high purity thiophene at different temperatures. This generates a partial pressure of thiophene from 10 to 100 Torr.

The reactions were performed in a Quartz plug flow reactor which can be temperature and time controlled. Since O_2 greatly enhances the etching rate, high purity He was used first for at least 30 min to flush out the residual air and heat the sample to the reaction temperature. The reacting gases were admitted when the system achieved the reaction temperature. After reaction, the reacting gases were removed and the samples were cooled to room temperature in He. This procedure assured that there was no significant reaction caused by gaseous impurities.

After reaction, the samples were transferred to a Nanoscope II scanning probe microscope which could be operated in both STM and AFM modes with the same software system. All examinations were made in air at 300 K. For STM the constant height mode was used. The scanning rate was adjusted for best images as described previously (*22–25*).

The surfaces were first randomly imaged over a large range of 15 × 15 μm^2 in about 20 different regions for each sample. Those showing etched structures were closely scanned with lower Z ranges and slower scanning rates. Repeated vertical calibrations were made using the step height of

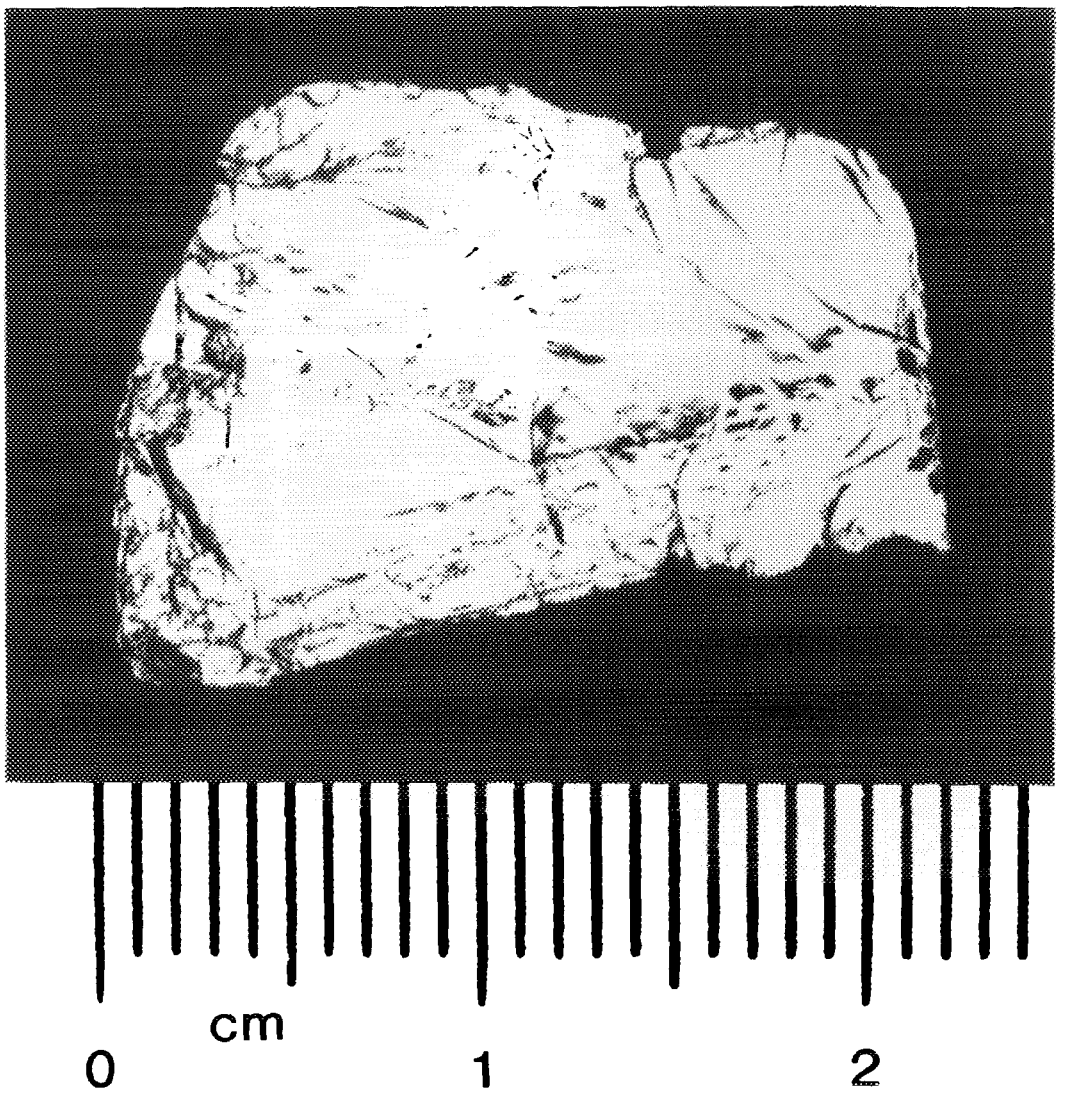

FIG. 1. An optical micrograph of a typical natural MoS_2 single crystal.

graphite. This instrument can easily distinguish monolayer from double or multilayer structures on the basal plane of MoS_2.

RESULTS

Low-Pressure Reactions

Figure 2a shows a region of a freshly cleaved surface of a MoS_2 single crystal. A monolayer patch caused by the cleavage is shown in the figure (the monolayer hereafter refers to the one sandwiched S–Mo–S layer (6.16 Å) in the MoS_2 crystal). Flat and defect-free regions with the dimensions of 20 × 20 μm were usually obtained by a single cleavage of the sample. This perfect surface provides a good reference for the surface microstructure changes after reaction.

Nearly triangular pits with a typical size between 300 and 500 nm randomly distributed over the surface of samples were found

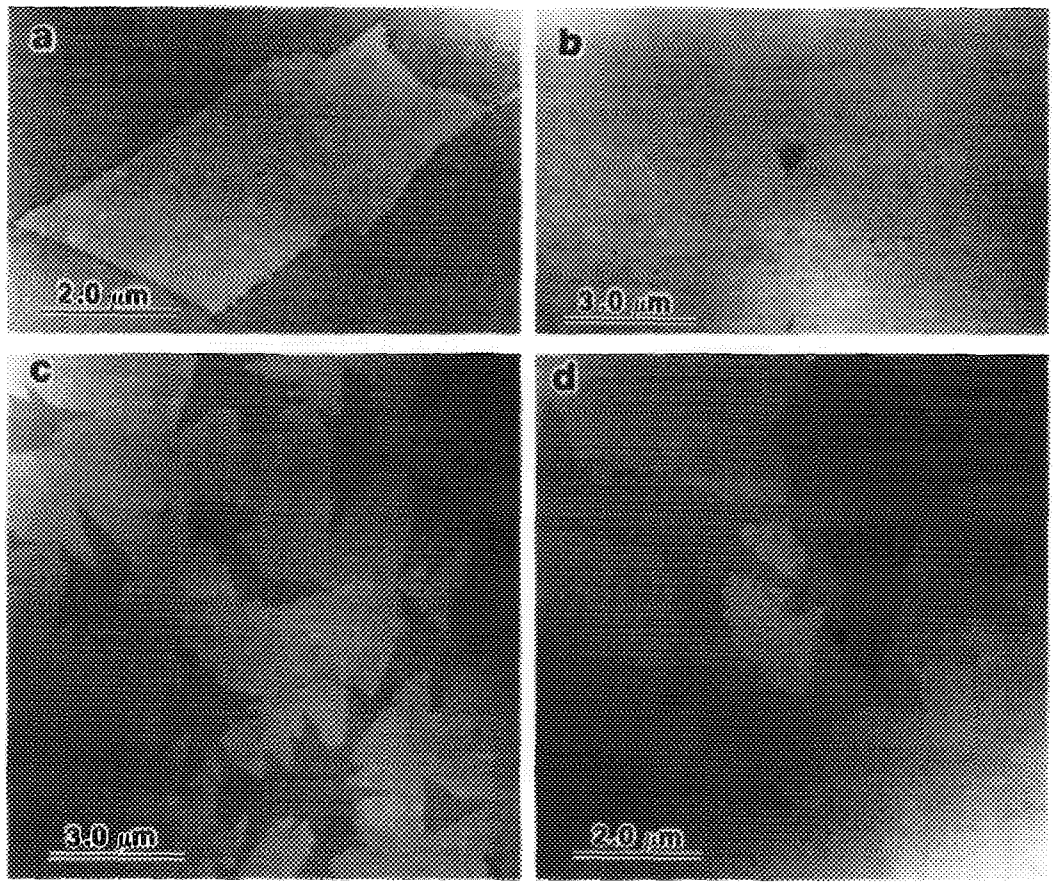

FIG. 2. STM images of etched surface structures after heating in 10% H_2 at different temperatures. (a) Unreacted surface with a monolayer patch, (b) triangular monolayer pit, after 60 min at 450°C, (c) tropical-fish-like monolayer pits, after 60 min at 550°C, and (d) double layer pit formed after 30 min at 600°C.

after heating in 10% H_2 at 450°C for 60 min. Figure 2b shows a low magnification view of such a monolayer triangular pit. The density of this type of pit is only about $10^6/cm^2$. The density depends on the region on the sample surface and increases with increasing temperature. This type of pit is probably generated from a basal plane vacancy similar to those observed in graphite gasification (*22–25*).

Figure 2c shows a sample after reaction in 10% H_2 at 550°C for 60 min. It can be seen that more of the top layer of the sample was removed, resulting in more irregular pits (but still generally triangular) which form tropical-fish-like shapes. These pits have several sharp corners along specific crystallographic directions. This probably reduces the total free energy of the system (the etched pits). All of these pits are exclusively one monolayer deep.

In addition to the monolayer patterns shown in Figs. 2b and c, other patterns were also observed at higher temperatures. Figure 2d shows a sample after heating in 10% H_2 at 600°C for 30 min; a double layer pit similar to those observed in graphite gasification is illustrated. The second layer pit

has the *opposite orientation* with respect to the first layer pit due to the alternating layer structure of MoS_2, which is similar to that observed in the NO_x–graphite reaction (*25*).

After some of the S atoms were gasified by H_2, the remaining Mo atoms could coalesce to form Mo particles. In STM examinations, Mo particles can be seen in the first few scans, but they are rapidly swept out by the STM tip due to the strong repulsive force between STM tips and metal particles and the weak adhesion force between Mo particles and the MoS_2 basal plane. This is very similar to the situation observed in catalytic gasification of graphite (*24*) using Pt and Rh as catalysts. However, AFM does not cause displacement of metal particles, and using AFM both the catalyst particles and the etched surface structures can be clearly evaluated.

Figure 3a shows a low-magnification view of an AFM image of the same sample as in Fig. 2c which was heated in 10% H_2 at 550°C for 60 min. Small Mo particles are randomly distributed over the surface. The particle are very uniform in size around 50 nm, and each of the Mo particles is nearly a cube. Figure 3b shows a high-magnification view of the same sample. It can be seen that each of the Mo particles is sitting on the edge of the monolayer step. It is evident that there are some kinks at the monolayer step (see the arrow in Fig. 3b). Mo particles probably move along and etch the edge during gasification.

At a higher temperature or longer reaction time, more sulfur atoms are removed and more Mo atoms are exposed, and this typically involves multilayers. Mo particles begin to coalesce to form larger Mo particles on the surface. We found that for small particles, the height is about the same as the horizontal dimensions, so each Mo particle forms either a rounded shape or a cube. However, large Mo particles resulting from reaction at high temperatures and/or longer reaction times are relatively flat, with the particle height much smaller than the particle size. In the MoS_2 structure, on the average each Mo atom is bound to two sulfur atoms, and the density of either Mo and S atom in the sandwiched layer is known to be 1.16×10^{15} atoms/cm^2. Therefore, by counting the size and density of the Mo particles formed in the reaction, we can estimate the amount of surface monolayer gasification. Table 1 shows the relative gasification rates of MoS_2 basal plane under various experimental conditions.

High-Pressure Reaction

Because hydrodesulfurization processes are usually carried out at high hydrogen pressures, we next extended the study of the reaction to 1 atm H_2 at different temperatures.

Figure 4a shows a sample after heating at 450°C in pure H_2 at atmospheric pressure for 40 min. It can be seen that the basal plane of the sample was abstracted by the reacting gas, resulting in many small pits. Most of these pits are one monolayer deep, while some of them are double layer. The sizes of these pits are in the range of 30 to 50 nm. The density of the pits is much higher than in the low pressure case, suggesting that at high pressure, direct abstraction of the sulfur atoms from the perfect site on the basal plane of MoS_2 is significant even at low temperatures. Figure 4b shows an amplified image of a region in the sample, showing a single pit consisting of many small patches. This indicates that the pit was probably expanded by the etching of the exposed Mo particles after initial opening.

Figure 5a shows a typical image of a sample after heating in pure H_2 at a high temperature of 550°C for 20 min. Flower-like structures are distributed over the surface. Most of them are one monolayer deep but a few expose multilayers. The density of the flower pattern is lower than that of low-pressure pits, suggesting that this kind of pattern is generated by the merging of the pits observed in Fig. 4.

Figure 5b shows a magnified image of a flower pattern in the same sample as in Fig.

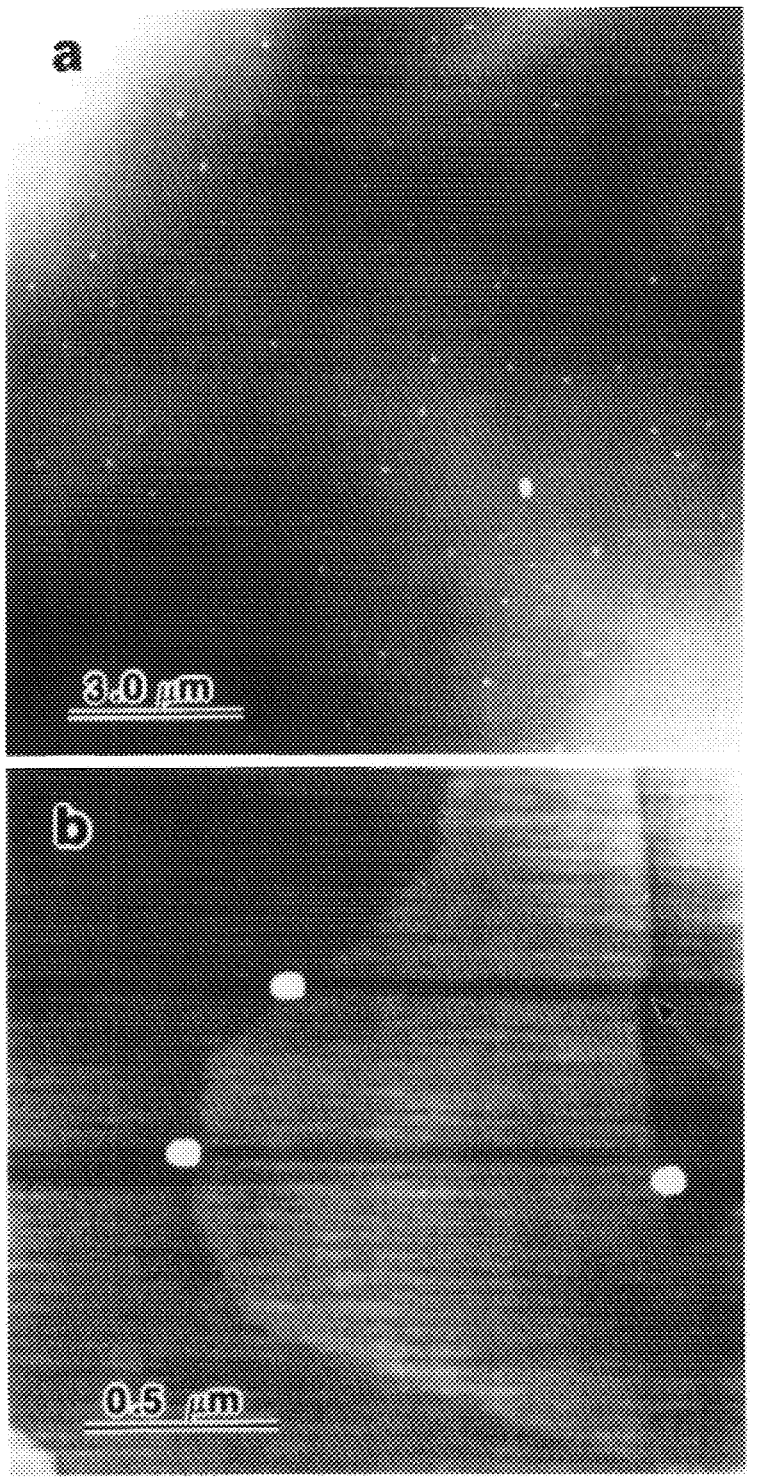

FIG. 3. AFM images of the same sample as in Fig. 2c. (a) Low-magnification view of surface showing uniform Mo particles and (b) enlarged view of (a) showing Mo particles stay at the edge of monolayer step.

TABLE 1

The Relative Rates for MoS_2 Basal Plane Gasification

Temperature (°C)	Etchant				
	0.1 atm H_2	1.0 atm H_2	0.1 atm H_2 with 30 Torr thiophene	0.1 atm H_2 with Ni and Co catalyst	150 Torr O_2
400					200–300
450	<1.0	50–70	<10	~40	>500
500	10–20	80–150	10–15	~100	
550	50–70	200–280			
600	80–150	300–450			

Note. 100 represents one S–Mo–S monolayer removal of the MoS_2 basal plane in 1 h.

5a. It extends along several directions on the surface. Figure 5c is a high-magnification view of the front of a flower pattern. Leaf-like patterns with streams, propagating toward the front of the pit, were created by the motion of many small Mo particles. Figure 5d shows a closer view at the front of the pattern. Small Mo particles sitting at the front are indicated.

At higher temperatures, Mo clusters were rapidly formed after the exposure of the Mo-layer and then moved radially. Figure 6 shows STM images of several regions of the reacted surface of a sample after exposure to a high temperature of 600°C for 20 min. In contrast to the low-temperature cases, many tiny channels are formed instead of large patterns. Also, it is interesting to notice that the channels formed a random pattern on the surface. The depth of these fine channels is varied from one to three monolayers (S–Mo–S layer).

Reactions with Thiophene

For any catalytic reaction, the real concern is the catalytically active sites at which the reaction takes place and the change with time. For the hydrodesulfurization reaction, the catalytically active sites are generally believed to be those at the sulfur vacancies or the atoms at the edges because significant differences in catalytic activities were found for the HDS on perfect and sputtered basal planes of MoS_2 single crystals (*32, 33*). One way to check the active site is to compare the etching rates of reactions with and without introducing a sulfur containing compound because, if the active sites are the edge sites, then the rate of etching will be hindered by the presence of this compound. This is simply due to the effect of sulfur deposition from thiophene balancing the removal of sulfur by hydrogen.

We introduced thiophene to the system because it is one of the sulfur-containing compounds in crude oil, and it is a liquid at room temperature, resulting in a wide range of partial pressures in an easily controllable temperature range. Because the formed monolayer pits are irregular in shape, it is difficult to quantify the rate of gasification as in the graphite gasification cases. However, as indicated previously, the amount of the Mo metal is directly proportional to the area of the sulfur atoms on the surface (i.e., the total rate of reaction). Therefore, by comparing the Mo particle sizes and density, we can estimate a qualitative rate of the gasification of the catalyst.

Figure 7a shows an AFM image of a sample after heating in 10% H_2 containing 30 Torr thiophene at 550°C for 30 min. The total fraction of the etched surface was estimated from the Mo particles to be about 26%. Figure 7b shows the Mo particle distribution in

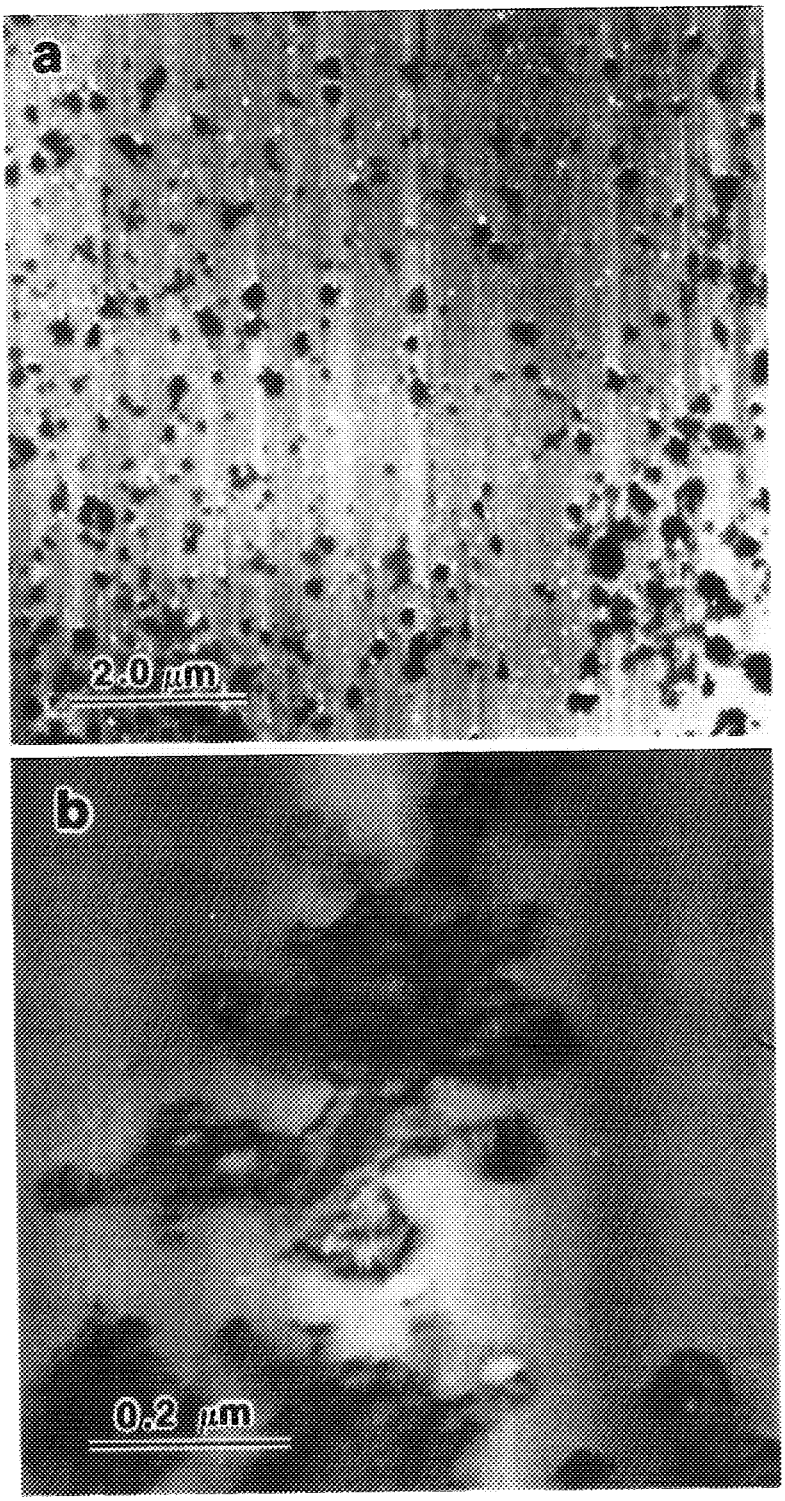

FIG. 4. STM images of a sample surface after heating in 1 atm hydrogen at 450°C for 40 min. (a) Low-magnification view showing small monolayer and multilayer pits randomly distributed over the surface and (b) enlarged image of the core region of a single pit.

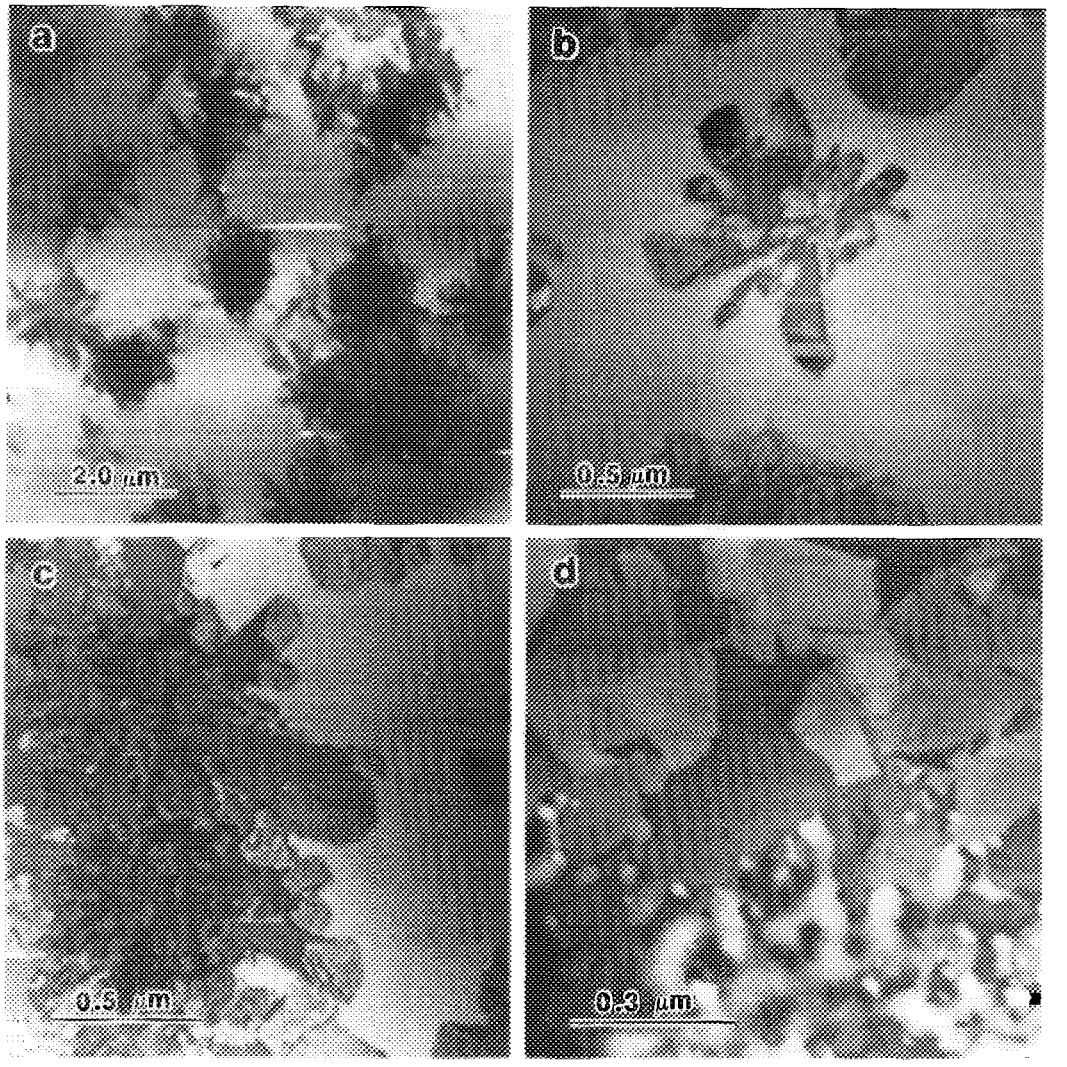

FIG. 5. STM images of flower-like patterns formed on a sample surface after heating in 1 atm hydrogen for 20 min at 550°C. (a) Low-magnification view showing the flower patterns randomly distributed over the surface, (b) enlarged view of a single flower pattern on the surface, (c) enlarged image of a region of the front of a flower pattern showing streams, and (d) details of the front of a flower pattern showing small Mo particles.

a sample after treatment at the same temperature and time with only 10% H_2 in the reacting stream (i.e., partial hydrogasification). It is evident that the number and size of the Mo particles were significantly higher than those in Fig. 7a, which corresponds to the hydrodesulfurization reaction (reaction after adding thiophene). The estimated gasification rate of the surface is about 57%. This suggests that the active sites in hydrodesulfurization reaction are indeed the edge sites along the monolayer steps on the MoS_2 surface.

Ni- and Co-Catalyzed Reactions

It is well known that the presence of a second metal in some cases produces a catalyst which has activities greater than the

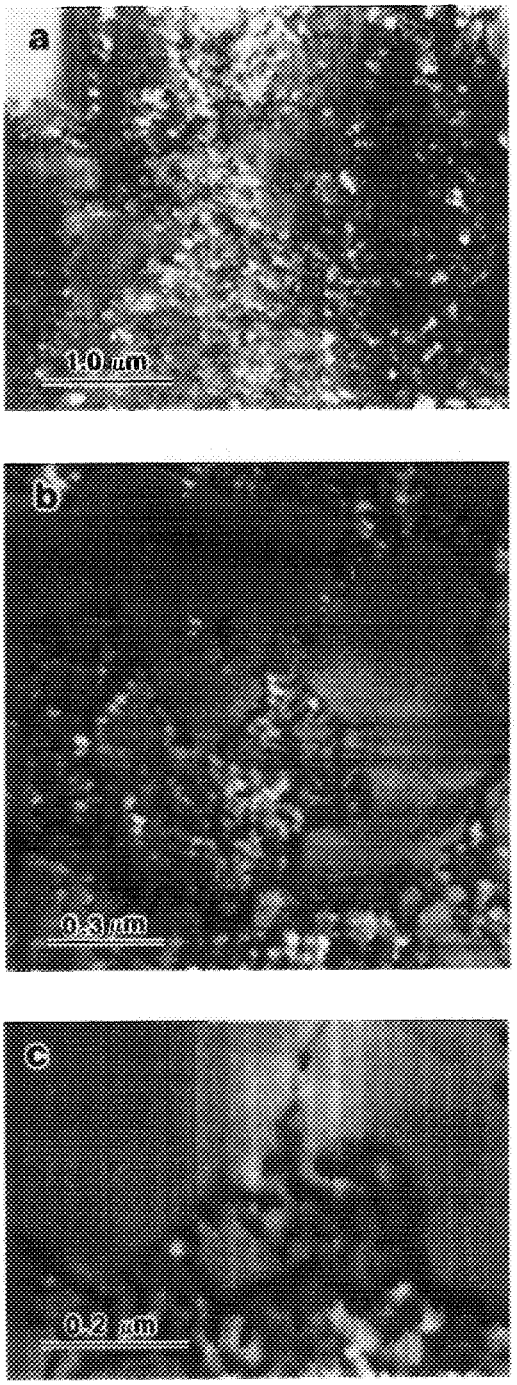

FIG. 6. STM images of irregular patterns formed on a sample surface after heating in 1 atm hydrogen at 600°C for 20 min. (a) Low-magnification view showing the pattern over the entire surface and (b) and (c) enlarged images show the front of the pattern which consists of many tiny channels carved by Mo particles.

simple sum of the activities of the catalysts. Such promotion of MoS_2 or WS_2 by Co or Ni in both supported and unsupported catalysts has been widely reported (*34*).

In this study, we introduced Co and Ni by depositing 20-Å thin films on freshly cleaved MoS_2 surfaces. The samples were then heated in high purity He at 450°C for 2 h to convert the metal films to small metal particles. After this, the samples with and without metals were heated in the same reactor at the same conditions.

Figure 8a shows a STM image of a sample surface after heating in 10% H_2 at 500°C for 30 min. In an area of about 15 × 15 μm, there are only two monolayer pits. These two pits were formed from some defect sites on the original surface described previously. Figure 8b shows an AFM image of the formed Co particles after the sample was heated in pure He at 450°C for 2 h. It can be seen that the whole surface is covered by the Co particles with a uniform size around 50 nm.

Figure 8c shows a STM image of the surface of sample covered by Co particles after heating in 10% H_2 at 500°C for 30 min. The whole sample surface is now decorated with many tiny triangular monolayer pits with sizes from 200 to 500 nm. It should be noted that during the first few scans of this region, the Co particles were still visible, but after several scans the Co particles were swept away by the STM tip. Figure 8d shows the surface of the sample with Ni particles after heating at 500°C for 30 min. The surface etching was also greatly enhanced by Ni particles. As the loading of Ni and Co and the effect of these two promoters are not exactly the same, it is difficult to compare their effects from the images. However, by comparing samples after reacting at different temperatures, it was evident that Co etched MoS_2 faster than Ni.

Evidently, the presence of either Co or Ni accelerates the formation of the monolayer pits on the basal plane of MoS_2. This explains the promotion effects of Co and Ni in hydrodesulfurization in a different way:

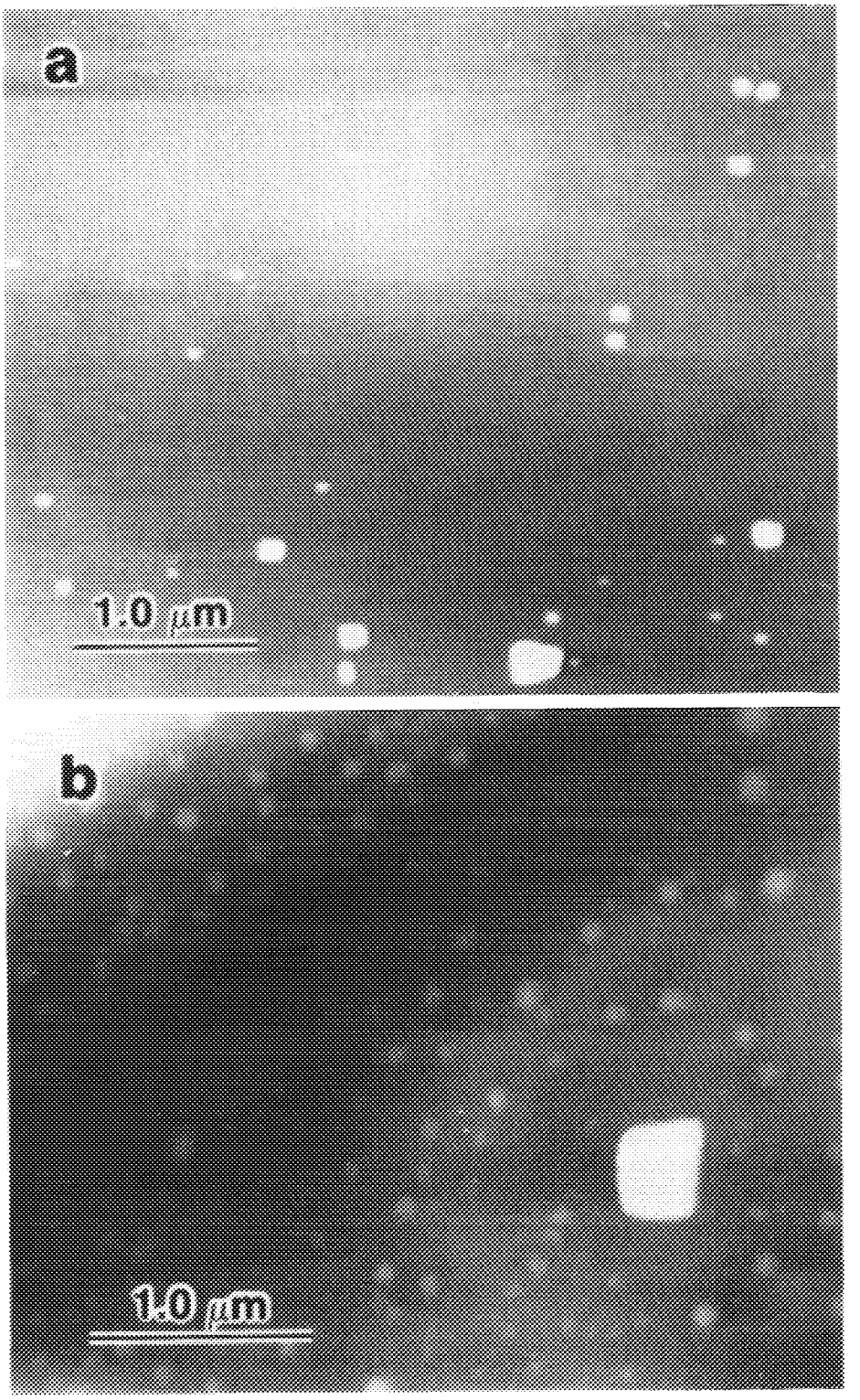

FIG. 7. AFM images of sample surfaces after heating in different gases at 500°C for 30 min: (a) 10% hydrogen and 30 Torr thiophene, low particle density; and (b) 10% hydrogen only, more Mo particles were formed.

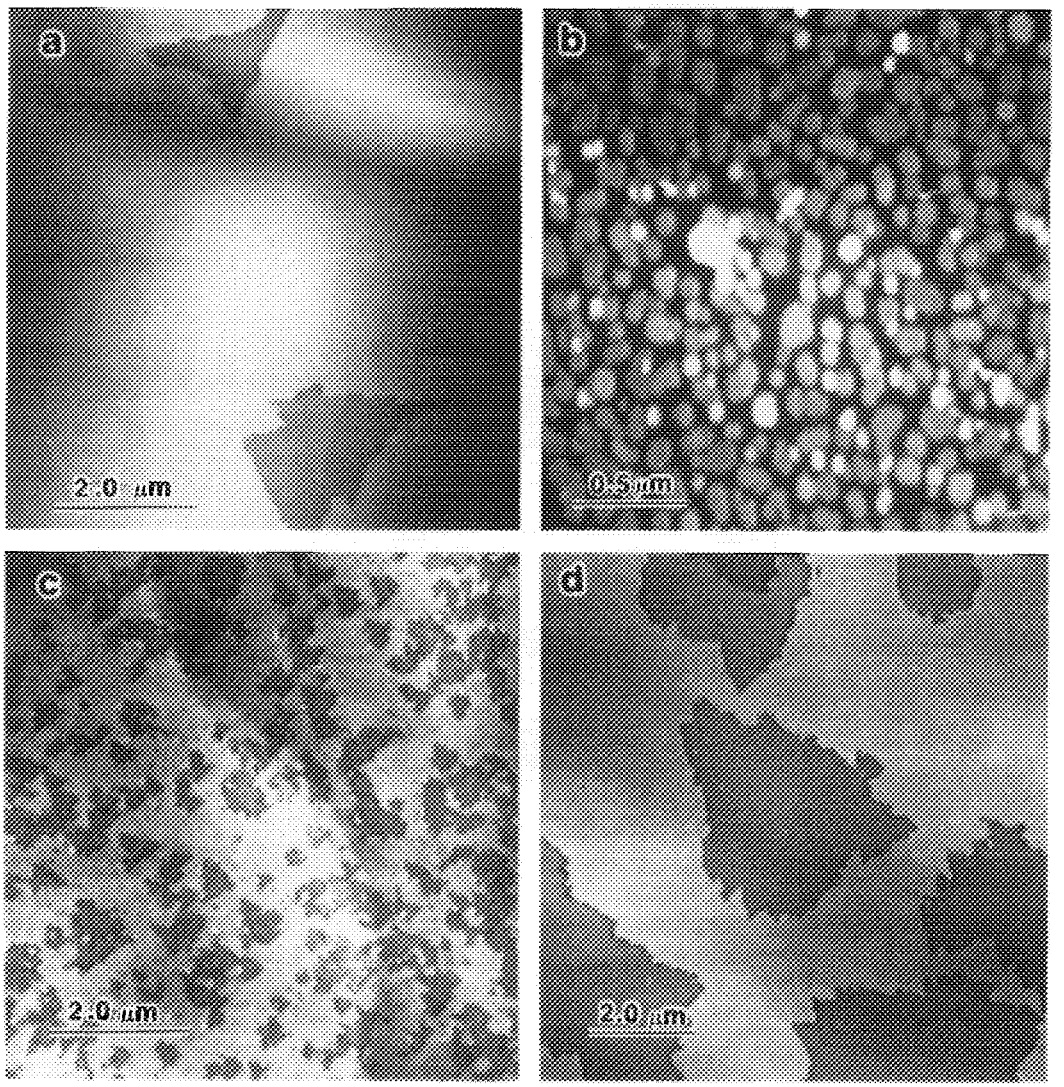

FIG. 8. STM and AFM images of samples with different catalysts after heating in 10% hydrogen for 30 min at 500°C. (a) Without Co or Ni, only two triangular monolayer pits formed over 10 × 10 μm region, (b) AFM image of Co particles on MoS_2 surface, (c) STM image of the etched surface after Co-catalyzed reaction showing randomly distributed triangular monolayer pits with a density much higher than that in (a), and (d) STM image of a sample surface after reaction catalyzed by Ni, showing big triangular pits and 80% of the surface reacted compared with 10% in (a).

Co or Ni acts as a catalyst in the process to accelerate the gasification of the top sulfur layer and thus produce more edge atoms, which are probably the catalytically active sites. It should be mentioned that the surfaces of Co and Ni particles might be converted to sulfides, especially at high temperature.

Oxidation of MoS_2

Hydrotreating catalysts are manufactured with metals (Mo, Ni, Co, etc.) as oxides. These metals must be converted to the presulfided state in order to achieve the desired activity and selectivity. Though the catalytic operation of MoS_2 is in a reducing at-

mosphere, the regeneration of the catalyst involves oxidizing the catalyst. Therefore, it is important to study the oxidation processes to get insight into the catalytic preparation and regeneration processes in order to monitor the morphologies, structures, and active sites.

MoS_2 and its oxidation were studied in the late 1960s by the Thomas group using the gold decoration TEM method from the crystal defect point of view (*8, 9*). Triangular rings with different orientations and configurations were observed after reaction in oxygen and decoration. They found that each of the rings was a monolayer pit resulting from the recession of a point defect on the surface of MoS_2 during oxidation. It is understood that sulfur became SO_2 and evaporated in this process. However, there remained the question of where the Mo goes. Recently, AFM has been used to study the oxidized surface of MoS_2 after heating in pure oxygen from the wear point of view because MoS_2 is a solid lubricant (*28, 29*).

We found that MoS_2 is very sensitive to O_2 even at low temperatures and therefore we conducted MoS_2 oxidation at lower oxygen pressures in the 30 to 150 Torr range. Figure 9a shows a sample after heating at 400°C for 10 min in 150 Torr oxygen. Many small MoO_3 crystals were formed on the sample surface. The crystals form mostly hexagonal shaped thin sheets. Figure 9c shows the sectional view of Fig. 9a. The height of the crystals is only one-tenth of the size of MoO_3 particles. Measurements of the individual crystals on the surface show that their heights are in a narrow range of 45 to 55 nm.

Figure 9b shows a low magnification view of a multilayer step region of the same sample as in Fig. 9a. It is noteworthy that big crystals were formed along the step. This is because the multilayer recession provides more Mo atoms to form big crystals. Figure 9d shows a sample after heating in 100 Torr oxygen at 500°C for 10 min. Considerably more MoO_3 crystals were formed on the sample surface. Atomic steps and twin structures in some small crystals are distinguishable in some regions.

DISCUSSION

Several models of hydrodesulfurization have been proposed thus far. In the solid-state chemistry model, it is assumed that the catalytically active sites was (1) a Mo ion located at the edge of a MoS_2 crystallite or (2) a basal plane sulfur vacancy (*30, 31*). In this model the desulfurization starts by adsorption of the sulfur atom of the reacting molecule on the sulfur vacancy. Hydrogen is believed to be used in a reductive addition reaction on sulfides (*35*). Two different configurations of the thiophene molecules during reaction were proposed: first, the one-point (end-on) mechanism in which the thiophene is assumed upright on the surface (*34*), and, second, the mechanism in which the adsorption of thiophene takes place via multipoint (side-on) adsorption (*36*).

A totally different mechanism was proposed based on surface analysis of a single crystal of Mo. A series of thiophene desulfurization studies on the Mo(100) single-crystal surface combined with surface science techniques for the characterization of substrate and adsorbates has been carried out (*37*). They found that thiophene dissociatively adsorbs on the surface of Mo(100). At low coverages, the molecules were flat on the surface, while they stood perpendicular to the surface at high coverages.

Our experiments on larger single crystals should be representative of the real situation because in the industrial catalyst large patches are formed on Al_2O_3. We found two fundamental processes during the catalytic operation: first, the surface sulfur layer is removed from some defect sites on MoS_2 basal plane to form monolayer pits, and, second, the exposed Mo layer forms small clusters which catalyze the further gasification of the sulfur layer, thus greatly enhancing the number of edge atoms.

At low reaction pressures, these two processes remove mainly the top sandwich

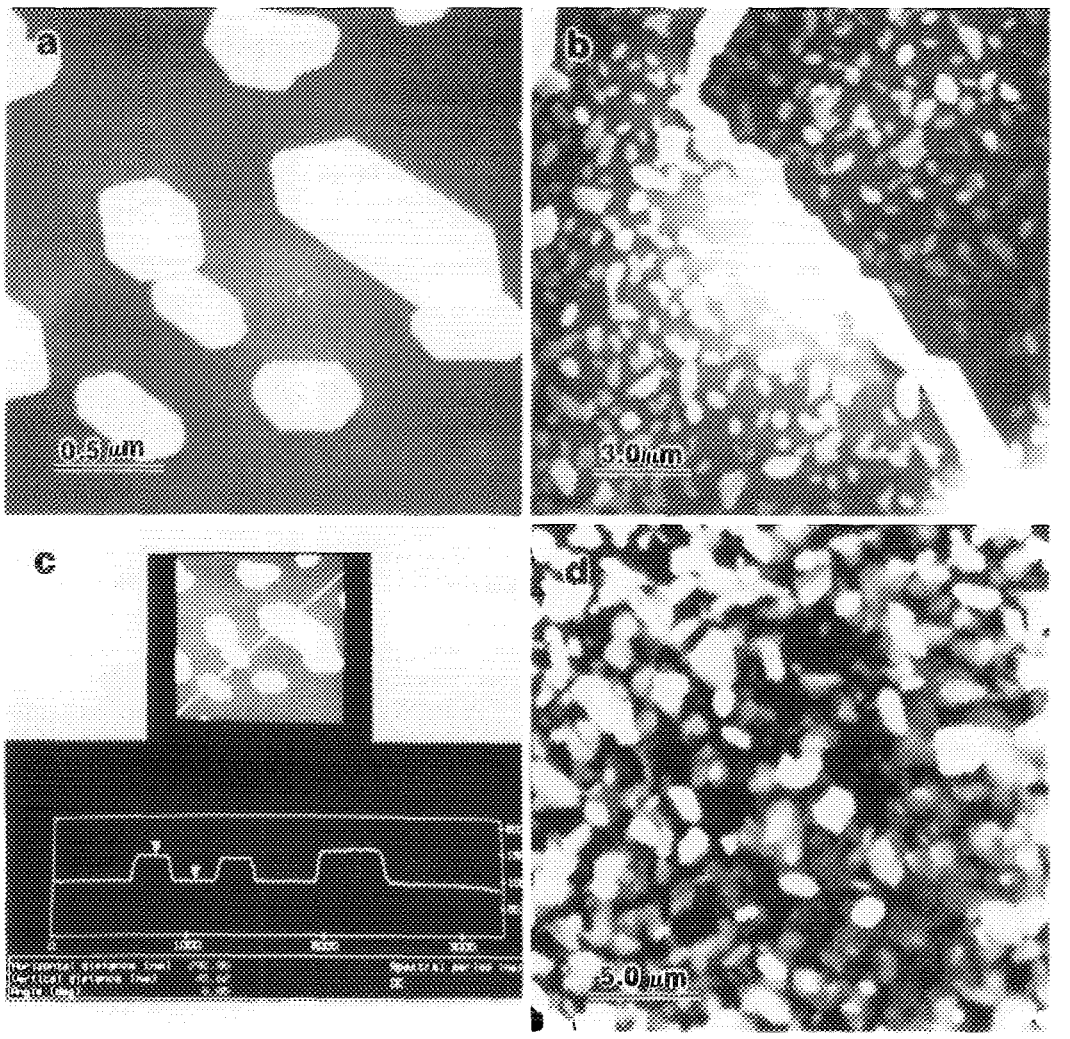

FIG. 9. AFM images MoO_3 particles formed on MoS_2 surface after heating in oxygen at different temperatures for different times: (a) in 150 Torr oxygen at 400°C for 10 min showing perfect flat hexagons with thickness of one or two monolayers; (b) the same as (a) showing large crystals formed at an edge; (c) sectional view of (a) showing that the height of the formed crystals is only about one-tenth of the width; and (d) higher density MoO_3 particles formed after 500°C for 10 min.

layer, and no Mo particles channeling into the upper sulfur layer were observed. However, at high pressures, the gasification is dominated by the rapid motions of the Mo particles, which produce high-density channel structures on the surface.

We find that thiophene retards the gasification of MoS_2. This suggests that the real hydrodesulfurization process was carried out at the edge sites. Sulfur deposition by thiophene balanced some of the sulfur removal by hydrogen. Therefore, the active sites of the hydrodesulfurization reaction should be the edge atoms.

Our experiment supported the solid state chemistry model with minor modifications.

Although the similarity in product distribution was found in the surface science studies, it should be noted that the activity of single crystal MoS_2 was measured at 1.0 atm compared to Mo (100) at 10^{-10} Torr, and we observed the remarkable difference in MoS_2 gasification at different pressures.

It is well known that the catalytic activity of a MoS_2/Al_2O_3 catalyst is strongly enhanced by addition of Co or Ni. Several different models have been proposed, among them: the introduction of Co (or Ni) increases the number of active sites, and, second, Co (or Ni) acts as a modifier of the active sites. The first category involves Co (or Ni) acting [**a**] as a textural promoter, [**b**] as a hydrogen spillover promoter, or [**c**] as a producer of new catalytic sites.

In model [**a**], the increase in the activity of the catalyst is attributed to an increase in the number of Mo sites at the catalyst surface. The role of the promoter is then textural. By altering the texture of the catalyst surface, the promoters create more active sites, without otherwise being involved in the catalytic activity. The location of the promoter was believed to be either between the sandwich layer (*30*), or at the edge of the MoS_2 crystals, not between MoS_2 layers, but in the MoS_2 layers, in the plane of the Mo cations (*4*).

In the hydrogen spillover model [**b**], Co or Ni forms a sulfide which provides hydrogen atoms to MoS_2. These spillover H atoms would create reduced centers on the MoS_2 surface which would be the catalytically active sites. Also, it has been proposed that the sulfides of Co and Ni themselves acts as new catalytic active sites (*38*). Thus the activity of the catalyst increased. A different mechanism is proposed in which Co (or Ni) acts as a modifier of the active sites (*3*).

Our experiments show that the active sites are edge atoms, and the presence of Ni and Co greatly enhances the number of edge atoms due to the catalytic gasification of MoS_2 by these metals. This strongly supports model [**a**]. This catalyzed process may involve the transfer of hydrogen through the metal particles as those in graphite gasification (*22–24*). Therefore, the spillover model is also possible.

SUMMARY

In conclusion, we have studied the dynamic behavior of MoS_2 gasification in the hydrodesulfurization process. The surface structure changes on MoS_2 during this process are influenced by reaction temperature, pressures, and catalyst composition. We found that two fundamental processes occurred on MoS_2 surface during the catalytic operation: first, the surface sulfur layer is removed from some defect sites on the MoS_2 basal plane to form monolayer pits, and, second, the exposed Mo layer forms smaller clusters which catalyze the further gasification of the sulfur layer, thus enhancing the number of edge sulfur atoms. Adding thiophene to hydrogen retards the gasification of MoS_2, suggesting that the active catalytic sites are the edges of the steps on the surface. Ni and Co were found to catalyze the gasification of MoS_2, and the number of the total active sites was then greatly enhanced.

ACKNOWLEDGMENTS

This research was sponsored by NSF under Grants CBT-882745 and INT-9000511, and by a grant from Ford Motor Company. STM and AFM images were obtained using facilities of the Center for Interfacial Engineering at the University of Minnesota. MoS_2 single crystals provided by Professor Z.D. Lin at the Institute of Physics, Chinese Academy of Sciences, and help from T. Tu are appreciated.

REFERENCES

1. Behbahany, F., Sheikhrezai, Z., Djalali, M., Salajeghen, S., *J. Catal.* **63,** 285 (1989).
2. Sanders, J. V., and Pratt, K. C. *J. Catal.* **67,** 331 (1981).
3. Chianelli, R. R., *Catal. Rev.-Sci. Eng.* **26,** 361 (1984)
4. Topsøe, H., Clausen, B. S., Topsøe, N., and Zeuthen, P., *in* "Catalysts in Petroleum Refining 1989" (D. L. Trimm *et al.* Eds.). Elsevier, Amsterdam, 1990.
5. Topsøe, H., and Clausen, B. S., *Catal. Rev.-Sci. Eng.* **26,** 395 (1984).

6. Delmon, B., *in* "Catalysts in Petroleum Refining 1989" (D. L. Trimm *et al.*, Eds.). Elsevier, Amsterdam, 1990.
7. Prins, R., De Beer, V. H., and Somorjai, S. A., *Catal. Rev.-Sci. Eng.* **31,** 1 (1989).
8. Bahl, O. P., Evans, E. L., and Thomas, J. M., *Surf. Sci.* **8,** 473 (1967).
9. Bahl, O. P., Evans, E. L., and Thomas, J. M., *Proc. Roy. Soc. London Ser.* **A 306,** 53 (1968).
10. Yang, R. T., and Yang, K. L., *J. Catal.* **90,** 194 (1984).
11. Stupian, G. W., and Leung, M. S., *Appl. Phys. Lett.* **51,** 1560 (1987).
12. Sarid, D., Henson, T. D., Armstrong, N. R., and Bell, L. S., *Appl. Phys. Lett.* **52,** 2252 (1988).
13. Weimer, M., Kramar, J., Bai, C., and Baldeschwieler, J. D., *Phys. Rev.* **B 37,** 4292 (1988).
14. Weimer, M., Kramar, J., Bai, C., and Baldeschwieler, J. D., *J. Vac. Sci. Technol.* **A 6,** 336 (1988).
15. Ichinokawa, T., Ichinose, T., Tohyama, M., and Itoh, H., *J. Vac. Sci. Technol.* A 8, 500 (1990).
16. Youngquist, M. G., and Baldeschwieler, J. D., *J. Vac. Sci. Technol.* **B 9,** 1083 (1991).
17. Heckl, W. M., Ohnesorge, F., Binning, G., Specht, M., and Hashmi, M., *J. Vac. Sci. Technol.* **B 9,** 1072 (1991).
18. Bailey, J. M., and Schmidt, L. D., *in* "Proceedings of the 47th Annual Meeting of the Electron Microscopy Society of America." San Francisco Press, San Francisco, 1989.
19. Porte, L., Richard, D., and Gallezot, P., *J. Microsc.* **152,** 515 (1988).
20. Chang, H., and Bard, A., *J. Am. Chem. Soc.* **112,** 4598 (1990).
21. Chang, H., and Bard, A., *J. Am. Chem. Soc.* **113,** 5588 (1991).
22. Chu, X., and Schmidt, L. D., *Carbon* **29,** 1251 (1991).
23. Chu, X., and Schmidt, L. D., *Surf. Sci.* **268,** 325 (1992).
24. Chu, X., Schmidt, L. D., Chen, S. G., and Yang, R. T., *J. Catal.* **140,** 543 (1993).
25. Chu, X., and Schmidt, L. D., *Ind. Eng. Chem. Res.* **32,** 1359 (1993).
26. Parkinson, B., *J. Am. Chem. Soc.* **112,** 7498 (1990).
27. Delawski, E., and Parkinson, B. A., *J. Am. Chem. Soc.* **114,** 1661 (1992).
28. Kim, Y., Huang, Jin-Lin, and Lieber, C. M., *Appl. Phys. Lett.* **59,** 3404 (1991).
29. Kim, Y., and Lieber, C. M., *Science* **257,** 375 (1992).
30. Voorhoeve, R. J. H., and Stuiver, J. C. M., *J. Catal.* 228 (1971).
31. Farragher, A. L., *Adv. Colloid Interface Sci.* **11,** 3 (1979).
32. Salmeron, M., Somorjai, G. A., Wold, A., Chianelli, R. R., and Liang, K. S., *Chem. Phys. Lett.* **90,** 105 (1982).
33. Farias, M. H., Gellman, A. J., Somorjai, G. A., Chianelli, R. R., and Liang, K. S., *Surf. Sci.* **140,** 181 (1984).
34. Lipsch, J. M., and Schuit, G. C. A., *J. Catal.* **15,** 179 (1969).
35. Ledoux, M. J., Michaux, O., Agostini, G., and Panissod, P., *J. Catal.* **102,** 275 (1986).
36. Kwart, H., Schuit, G. C. A., and Gates, B. C., *J. Catal.* **61,** 128 (1980).
37. Gellman, A. J., Neiman, D., and Somorjai, G. A., *J. Catal.* **107,** 92 (1987).
38. DeBeer, V. H. J., Duchet, J. C., and Prims, R., *J. Catal.* **72,** 369 (1981).